THE PROPERTIES AND ENVIRONMENT OF THE GIANT, INFRARED-LUMINOUS GALAXY IRAS 09104+4109

S. G. KLEINMANN
Department of Physics and Astronomy, University of Massachusetts

DONALD HAMILTON
National Optical Astronomy Observatories[1]

W. C. KEEL
Sterrewacht, Leiden

AND

C. G. WYNN-WILLIAMS,[2] S. A. EALES, E. E. BECKLIN,[2] AND K. D. KUNTZ[2]
Institute for Astronomy, University of Hawaii
Received 1987 August 7; accepted 1987 October 26

ABSTRACT

IRAS 09104+4109 is the most luminous object yet discovered by means of the *IRAS* survey. It is identified with a cD galaxy having a strong emission-line spectrum at a redshift of 0.442 and emits $6 \times 10^{12} L_\odot h^{-2}$, 99% of which emerges at infrared wavelengths. One component of a double radio source is coincident with the center of the galaxy. The high luminosity of this source may be related to an interaction with one or more members of the rich cluster in which it lies. There is a secondary peak in the emission-line image of the galaxy. Emission lines from both regions are broad (~ 900 km s^{-1}) but narrower than those characteristic of the only other objects known to have such high luminosities, such as Seyfert 1's and QSOs. It is suggested that the strong infrared excess of IRAS 09104+4109 is produced by dust obscuring a broad line region.

Subject headings: galaxies: clustering — galaxies: individual (IRAS 09104+4109) — infrared: sources

I. INTRODUCTION

Intensive studies of high-latitude sources detected by *IRAS* at 60 μm have shown that most of them can be identified with extragalactic objects and that some reach luminosity levels typical of QSOs. Houck *et al.* (1985) studied a group of optically faint ($m_{pg} > 18.5$) 60 μm sources and found that these objects could be identified with some of the most distant and luminous galaxies seen in the *IRAS* survey.

Exploiting the result that objects with high L_{IR}/L_B may have high infrared luminosities, we undertook a systematic search of a 530 deg^2 region ($9^h < \alpha < 14^h$, $+40° < \delta < +50°$) for 60 μm sources lacking strong optical counterparts. By searching the POSS plates in the vicinities of 305 sources from the *IRAS* Point Source Catalog (1985) in the selected region having $F(60) > 0.5$ Jy and nonstellar colors [i.e., no detection at 25 μm or $F(25)/F(60) < 3$], we obtained a list of 10 that had no optical counterpart brighter than 18th mag. Spectra of the faintest three of these resulted in the discovery of the most distant object found yet as a result of the *IRAS* survey, IRAS 09104+4109. This source is also distinguished by having the "warmest" infrared colors [in the sense of a high ratio of $F(25)/F(60)$] of any of the objects detected at both 25 μm and 60 μm in our optically faint sample. De Grijp *et al.* (1985) showed earlier that a large fraction of infrared sources with spectral indices flatter than -1.5 between 25 and 60 μm could be identified with Seyfert galaxies.

A preliminary report on the properties of this object was given by Kleinmann and Keel (1987; hereafter KK). These authors noted that *IRAS* 09104+4109 fell between two ~ 18th mag optical objects, one of which—the source they labeled "Object 1"—had an emission-line spectrum at a redshift of $z = 0.442$. Their "Object 2" was also interesting since it appeared to sit nearer than Object 1 to the center of a rich cluster of galaxies.

In this paper, we present ground-based infrared measurements that demonstrate unambiguously that it is Object 2, not Object 1, that should be identified with the *IRAS* source. New imaging and spectroscopic observations show that the previously reported emission-line spectrum *is really that of Object 2*. The new data fortify the earlier speculation that Object 2 is physically associated with the apparent cluster in which it lies and demonstrate its similarity in optical luminosity and extent to other galaxies dominating rich clusters.

II. OBSERVATIONS

a) Infrared Photometry

Improved *IRAS* photometry of IRAS 09104+4109, obtained by co-adding all of the available survey data, was presented by KK. For convenience, it is summarized in Table 1. We emphasize here that the statistical significance of the upper limit quoted at 100 μm is unclear, since strong fluctuations in the baseline are produced by the emission of cool diffuse high-latitude clouds in the Galaxy (the so-called infrared "cirrus"; Low *et al.* 1984).

In 1986 November the Infrared Telescope Facility (IRTF) was used with the facility bolometer to measure the 10 μm emission from each of the potential optical counterparts

---

TABLE 1

PHOTOMETRY OF IRAS 09104+4109

Wavelength	Band	Telescope	Flux density (mJy)
0.445 μm	...	KPNO 4 m	0.080 ± 0.005
0.555 μm	...	KPNO 4 m	0.080 ± 0.005
0.64 μm	...	KPNO 4 m	0.090 ± 0.005
0.79 μm	...	KPNO 4 m	0.180 ± 0.005
1.25 μm	J	IRTF	0.43 ± 0.04
1.65 μm	H	IRTF	0.65 ± 0.07
2.2 μm	K	IRTF	0.87 ± 0.09
3.8 μm	L'	IRTF	2.6 ± 1.3
10.1 μm	N	IRTF	88 ± 17
20 μm	Q	IRTF	270 ± 70
12 μm	...	*IRAS*/IPAC	170 ± 30
25 μm	...	*IRAS*/IPAC	390 ± 30
60 μm	...	*IRAS*/IPAC	550 ± 50
100 μm	...	*IRAS*/IPAC	<390
6 cm	...	VLA	1.8 ± 0.3
20 cm	...	VLA	6 ± 1

described by KK. A clear signal of 88 ± 17 mJy was detected through an 8″ diaphragm centered on the optical image of Object 2, but only 26 ± 26 mJy from Object 1. Subsequent 1.2–20 μm photometry of Object 2 with an 8″ diaphragm is listed in Table 1. The agreement between the *IRAS* and IRTF flux densities in the 10–25 μm range is good enough that we can conclude that at least 70%, and probably all, of the emission from IRAS 09104+4109 originates from Object 2. Table 2 shows the *IRAS* and optical positions of the source; the position of the optical centroid of the source was measured on the glass copy of the O plate of the POSS, using the two-axis Grant measuring engine at NOAO.

b) Optical Imaging Data

In order to study the morphology of the optical counterpart of IRAS 09104+4109, and of the cluster of galaxies surrounding it, we have obtained new deep R and I images of the region, using the KPNO 2.1 m telescope with the RCA1 CCD. All observations had a scale of 0″.38 pixel^{-1}, and therefore, covered a 192″(EW) × 120″(NS) field-of-view. On 1987 February 1 (UT), we obtained a series of images of the optical counterpart of IRAS 09104+4109, consisting of three exposures each in R and I Mould filters and two through an 80 Å wide interference filter centered at 7240 Å. In the rest frame of IRAS 09104+4109, the interference filter covered the spectral region 4992–5047 Å, thus bracketing the [O III] emission. The R exposures were 900 s each; the I and 7240 Å frames were

TABLE 2

POSITIONS OF SOURCES NEAR IRAS 09104+4109

Designation	R.A. (1950)	Decl. (1950)
IRAS 09104+4109 ...	9^{h}10^{m}29^s.8[a]	+41°09′04″[a]
Object 2	9 10 32.92[b]	+41 08 52.4[c]
Radio source	9 10 31.86[c]	+41 08 53.2[c]

[a] The *IRAS* position for this source has an uncertainty ellipse of dimensions 11″ × 24″ at P.A. 108°.

[b] The optical position for this source was measured at the two-axis Grant measuring engine at NOAO, using the KPNO glass copies of the Palomar Observatory Sky Survey. The 1 σ error in the fit of 10 measured reference stars to their cataloged coordinates is 0″.5.

[c] The radio position measured at the VLA has an estimated uncertainty in each dimension of 0″.5.

1000 s each. On the next night, we obtained three 600 s R images of fields 40″ north and three images south of IRAS 09104+4109. On both nights, the sky was photometric and moonless and the seeing varied between 1″.0 and 1″.5 (FWHM). All of these observations were obtained at an airmass less than 1.1.

The R and I images were calibrated by observations of nearly 20 standard stars ranging in (R−I) color from −0.20 to +1.2 taken from Landolt (1983). Each standard star was exposed three times on the CCD chip, but with the telescope offset 20″ between the exposures. All standard stars were observed at an airmass <2.0. The transformation equations to the Kron-Cousins system were obtained by a simultaneous nonlinear least squares solution of the instrumental and atmospheric parameterizations. This analysis showed that the difference in the photometric zero-point amounted to only 0.01 mag for R and 0.02 mag for I. The photometric precision at 22.0 mag is ~4% for the R photometry and ~7% for the I photometry. An image of the field is presented as a mosaic of R images of the region in Figure 1 (Plate 5). Contour maps of Object 2 in the R frame and "[O III]" frame are shown in Figures 2a and 2b, respectively. For comparison, a contour map of a stellar image found on the R frame is presented in Figure 2c.

Measurements of the morphology of Object 2 in the R images were made with the GRASP surface photometry package written by M. Cawson (see Davis *et al.* 1985), by fitting ellipses to isophotes at stepped major axis sizes. This analysis showed that the object has an extensive envelope, whose brightness measurably exceed that of the sky at radii up to 12″ from the central core, where it has a surface brightness of 26.0 mag arcsec^{-2}. On the [O III] image, the galaxy does not appear to be significantly extended, except for the appearance of a secondary maximum, which has 10% of the peak intensity of the core and is located at P.A. 25°.

Measurements of the brightnesses of other objects found in the deep R and I images centered on IRAS 09104+4109 were made with the Kitt Peak version of FOCAS (Valdes 1982a, b). Magnitudes were obtained through a 12″.2 diameter aperture, chosen to maximize photometric accuracy but minimize the sky background. A complete catalog of sources brighter than R = 22 mag is given in Table 3, along with R mag, R−I color, and offset in arcsec from the optical counterpart of IRAS 09104+4109. The 1 σ statistical uncertainty in the R band photometry of the faintest sources is 0.04 mag. For sources fainter than R = 22 mag, the accuracy of the photometry and the completeness of the catalog were strongly affected by confusion. Cases where confusion biased the photometry of sources included in Table 3 by more than 20% are marked with a "C" in the table.

c) Optical Spectrophotometry

Spectrophotometry of Object 2 was obtained on two occasions. On 1986 March 1 (UT) we obtained two spectra with a spectral resolution of 15 Å from 5800 to 9100 Å. The exposure times were 1200 and 2400 s. The sky conditions were not photometric and the seeing was ~1″.5. On 1987 January 2 (UT) we obtained two spectra that cover the wavelength range 4500–7900 Å also with a spectral resolution of 15 Å. The exposure times were 1800 and 1200 s. The conditions during this latter run were excellent: there was no moon, the sky was photometric, and the seeing was 1″. In both sets of observations the cryogenic camera on the Mayall telescope was used
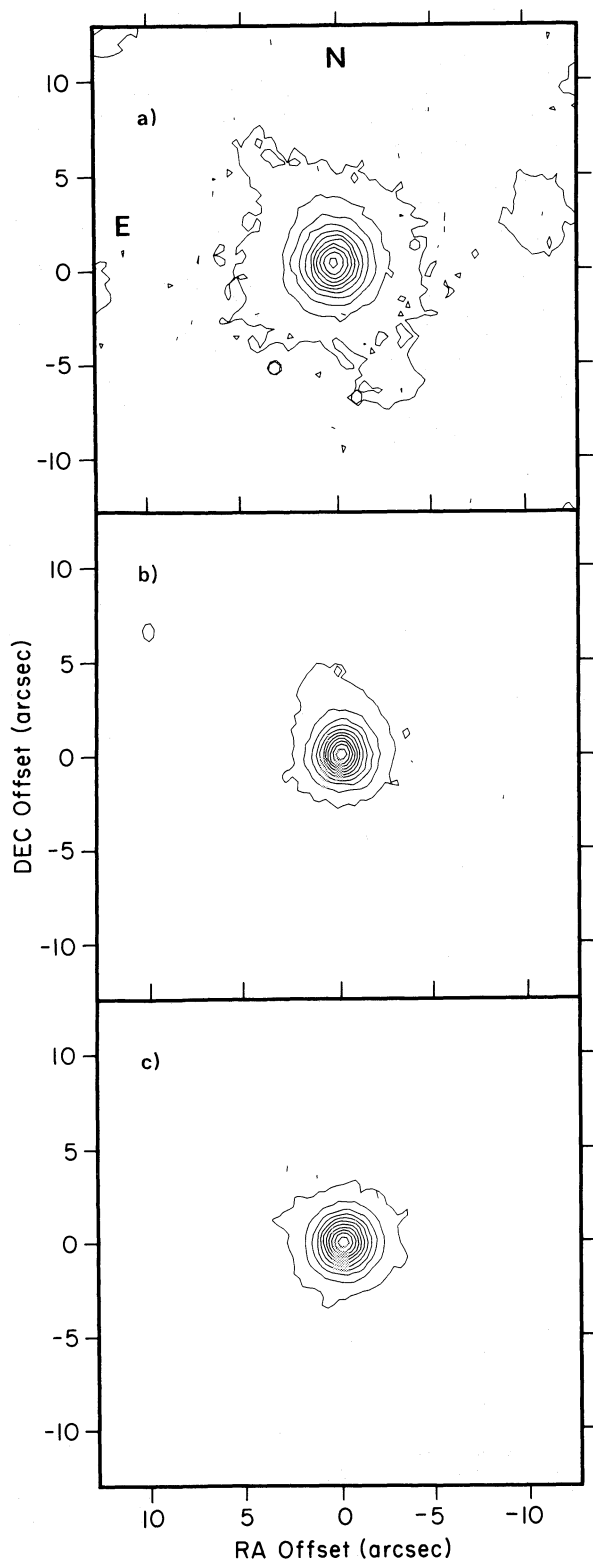
FIG. 2.—Contour maps derived from the CCD images. In all cases, the contour intervals are equally spaced by 9% of the peak intensity, and range from 3.5% (at the lowest contour) to 93.5% of the peak signal. (*Top*): *R* band image of the galaxy; (*middle*) narrow-band image of the galaxy, centered on [O III] 5007 Å in the rest frame of the galaxy; (*bottom*) *R* band image of a star taken from the same frame as the galaxy.

$\Delta\alpha^a$	$\Delta\delta^a$	R (mag)[b]	$R-I$ (mag)[b]
−112.9	−6.8	19.89	1.04
−112.1	−39.1	20.93C	0.29C
−111.7	29.3	21.22	0.80
−105.3	0.0	19.87	0.77
−95.8	−42.9	21.35	0.13
−90.4	−13.7	20.25	0.65
−88.9	−6.8	21.61	0.88
−87.4	−35.0	21.92	1.09
−82.8	17.5	21.97	1.27
−80.6	−3.4	21.09	0.62
−78.7	−16.3	20.31	0.55
−76.0	49.0	20.65	0.74
−75.2	−36.5	21.61	0.61
−73.3	−52.1	19.87	0.74
−72.6	−0.8	20.77	1.03
−67.6	2.7	20.90	1.59
−66.1	−16.7	19.99	0.79
−65.4	25.8	19.24C	0.97C
−65.0	20.1	19.29C	0.95C
−60.0	0.8	21.93	−0.03
−58.9	45.6	18.90	0.48
−57.8	−10.6	21.29	1.03
−54.7	−29.3	21.79	0.46
−50.9	7.2	20.17	0.70
−46.7	3.4	20.48C	0.93C
−42.6	29.3	18.42	0.42
−42.2	−7.6	21.90	1.50
−41.0	−48.3	20.29	0.61
−36.9	−15.6	20.00	0.89
−30.0	−9.5	20.38C	1.04C
−28.5	−6.8	20.37C	0.97C
−28.1	0.8	21.31C	−0.50C
−25.1	33.4	21.97	0.00
−22.0	−7.6	20.97	0.94
−18.6	26.6	20.58	0.98
−17.9	40.7	21.62	0.54
−16.0	1.1	20.80C	0.52C
−14.8	52.4	21.81	0.39
−13.7	−19.0	21.68C	0.43C
−12.9	8.7	20.82	0.51
−12.5	−13.3	21.27	0.38
−11.8	−47.5	21.97	0.85
−10.3	2.3	19.88C	0.00C
−3.0	−5.7	18.81C	0.70C
−0.4	−52.4	21.41	0.68
0.0	0.0	17.86	0.93
7.2	−37.6	21.49	0.00
12.2	12.2	20.16	1.01
12.9	−1.5	20.30	0.78
12.9	31.9	20.84C	0.89C
16.7	46.4	21.94	0.00
17.1	35.3	20.75	0.90
21.7	−11.8	21.35	1.11
25.1	5.7	19.99	0.84
31.2	16.0	20.65	1.40
34.2	−9.1	21.38	0.55
36.9	−39.9	20.87	0.66
39.1	17.9	21.80	0.92
49.0	−45.2	20.89	0.92
50.5	−21.3	21.26	1.05
55.5	−52.1	21.62	0.75
57.8	22.8	20.92	0.88
63.1	49.8	21.99	1.10
64.6	30.0	21.01	1.01
65.4	−19.8	21.71	1.05

[a] Offset in arcsec from the peak position of the optical counterpart of IRAS 09104+4109.
[b] Values marked "C" are uncertain due to confusion.

163

with a 2″.5 by 5′ slit. For the 1986 observations the slit was aligned east-west. In 1987 the slit was oriented at P.A. 35° for the 1800 s exposure, and north-south for the 1200 s exposure. All spectra were obtained at an airmass less than 1.3.

Observations of the standard stars of Oke and Gunn (1983) were obtained with the same instrumental setup except that the slit width was set to 10″.8 for better spectrophotometric accuracy. For the 1986 observations, this permitted the instrumental system to be placed on a relative energy system. For the 1987 observations, a transformation to absolute energy units was derived. All spectroscopic observations were reduced using the long-slit package in IRAF (Valdes 1986). The standard form and zero-point for the atmospheric extinction over Kitt Peak was assumed.

The combined calibrated spectrum is presented in Figure 3. Emission lines previously identified in the spectra of Seyfert galaxies by Cohen and Osterbrock (1981), Schmidt and Miller (1985), and Malkan (1986), and in the spectrum of Cygnus A by Osterbrock and Miller (1975) are listed in Table 4, along with their identifications, integrated fluxes, and equivalent widths. The average redshift deduced from the strongest Balmer and oxygen lines is 0.4417 ± 0.0002. The velocity difference between the high- and low-ionization lines is at most 200 km s^{-1}. In addition to these lines, we also observe strong unblended features near 5173 Å (probably He I 3587 Å), 6095 Å, and 7425 Å; the latter two features have a line profile that differs from the other lines in the spectrum. Notably, no permitted or forbidden Fe II emission lines were discerned in the spectrum. Ca V (5309 Å), also absent, has an excitation and ionization similar to many other lines in the spectrum, but falls in the atmospheric A band.

A number of lines in the spectrum are sufficiently strong that their profiles could be examined in detail. The strongest for-

TABLE 4

POSITIONS AND STRENGTHS OF OBSERVED EMISSION LINES

λ_{obs}	Identification	Flux[a]	E. W.[b]	Flux/Flux(Hβ)
4519......	3132.9 [O III]	5.4	2.0	0.045
4619......	3203.1 He II	6.3	5.3	0.053
4826......	3345.9 [Ne V]	17.6	10.3	0.15
4942......	3425.8 [Ne V]	57	33.2	0.48
5173......	3587.4 He I	2.9	2.1	0.024
5375......	3726/3729 [O II]	210	134.0	1.8
5577......	3868.7 [Ne III]	100:	91.9	0.83
5607......	3888.6 [Ne III] (+H ζ)	22	18.2	0.18
5720......	3965/8 [Ne III] (+H ε)	45	37.2	0.38
5867......	4069/4076 [S II]	10.5	8.0	0.088
5914......	4101.7 Hδ	24	18.2	0.20
6095......	4226.8	8	6.2	0.067
6259......	4340.5 Hγ	61	46.9	0.51
6292......	4363.2 [O III]	19	14.8	0.16
6452......	4471.5/4471.7 He I	5.9	4.4	0.049
6755......	4685.7 He II	23	14.6	0.19
7008......	4861.3 Hβ	120	72.0	1.0
7146......	4958.9 [O III]	490	295.2	4.1
7214......	5006.8 [O III]	1400	851.0	12.
7425......	5146.8	7.2	5.3	0.060
7496......	5198.5/5200.7 [N I]	6.8	5.0	0.057
8249......	5720.5 [Fe VII]	4.5	3.5	0.038
8473......	5875.6/5876.0 He I	11.3	8.6	0.094
8775......	6085.5 [Fe VII]	14.2	11.6	0.12
9085......	6300.2 [O I]	35.3	31.0	0.29
9177......	6363.9 [O I]	11.9	10.4	0.10

[a] Integrated line fluxes are given in units of 10^{-16} ergs cm^{-2} s^{-1}.

[b] The listed equivalent widths have been corrected by an amount $(1 + z)^{-1} = 0.69$ to the rest frame of the galaxy.

bidden lines, [O III] 4959 and 5007, have profiles similar to that of Hβ, the strongest permitted line in the spectrum. No broad line component is observed in Hβ. All of these lines are
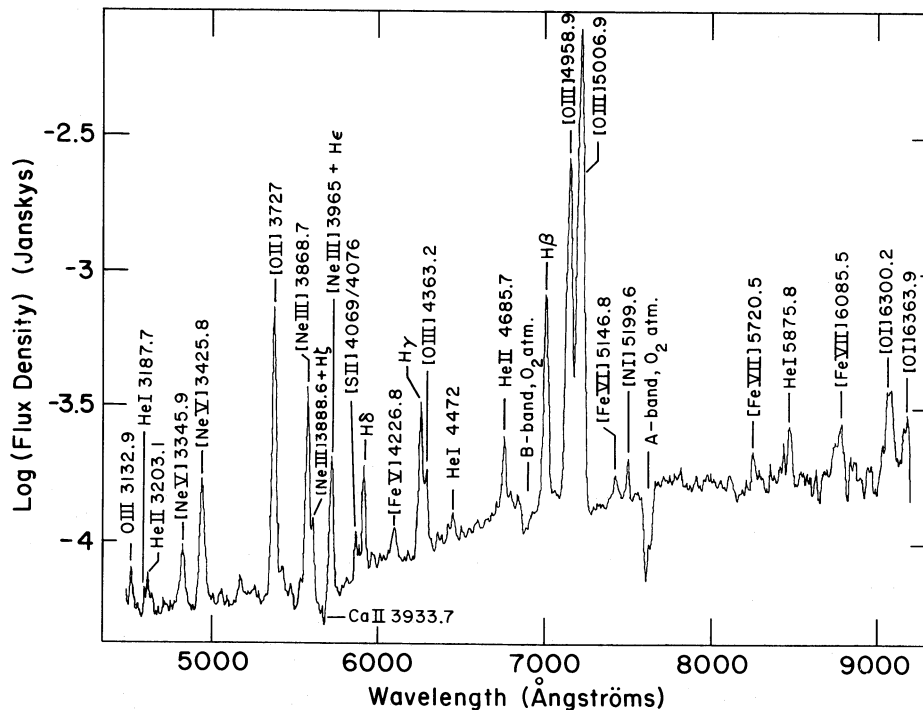

FIG. 3.—The calibrated optical spectrum of the galaxy identified with IRAS 09104+4109, presented in the observed rest frame. Markings distinguish the emission lines listed in Table 4, the Ca II K absorption line, and two residual atmospheric features.

asymmetric, in the sense that they have strong blue wings. The lines are well fitted by a combination of two Gaussians such that the blue component contains ~20% of the total flux in the line and is centered at −950 km s^{-1} relative to the velocity of the stronger component. The full width at half-maximum intensity of each of the two components is 20 Å, which, corrected for the instrumental profile and the redshift, corresponds to an intrinsic width of 600 km s^{-1} FWHM.

An additional search for a broadened component to the H lines was made by obtaining a longer wavelength spectrum of IRAS 09104+4109, covering the vicinity of the Hα line. This spectrum was taken with the faint-object spectrograph (FOS) at the 2.5 m Isaac Newton Telescope on La Palma on 1987 June 26. The spectrum covered the range 5200–10,000 Å, had a resolution of 20 Å, and a signal-to-noise ratio of 15 near Hα, but away from strong telluric OH lines. These data limit any broad (~100 Å) component to the Hα line to be less than that in the narrow component.

Since the slit of the cryogenic camera was oriented within 10° of the secondary maximum seen in the [O III] image, we could obtain preliminary information on differences between the spectrum at that position and at the core. We find no evidence for any difference greater than 1 σ in line widths at these two positions. However, the line ratios differ significantly. Relative to [O III] 5007, [O II] is stronger by a factor of 5, and Hβ is weaker by a factor of 2 at the secondary peak than at the nucleus.

A summary of the observed monochromatic flux densities of IRAS 09104+4109 is presented in Table 1. Evidence for a strong contribution from starlight to this continuum is provided by the detection of the Ca K line in absorption. This is the strongest stellar absorption feature seen in the optical spectra of normal galaxies. Other potentially detectable lines, notably Mg b 5175 Å and Na D 5892 Å are masked by the emission features 5146.8/5199.6 Å and He I at 5875.8 Å.

In the long slit spectra obtained with the cryogenic camera, we observed other galaxies simultaneously with that of Object 2. Two other galaxies were sufficiently bright to yield redshifts. The spectrum of a galaxy located at $\Delta\alpha = 75''$ E, $\Delta\delta = 0''$ from Object 2 contains the emission lines Hα and [O III] 5007 and is at a redshift of 0.30. The spectrum of the galaxy located at $\Delta\alpha = -105\rlap{.}''3$, $\Delta\delta = 0\rlap{.}''0$ from Object 2 has only absorption features; these occur at wavelengths consistent with their identification as the G band, CN at 4216 Å, Hβ, and Mg b in a spectrum redshifted by the same amount as Object 2, z = 0.442. Another galaxy in the field, at $\Delta\alpha = -58\rlap{.}''9$, $\Delta\delta = +45\rlap{.}''6$ from Object 2 was separately observed in 1987; it has emission-line features which yield a redshift of 0.12.

A spectrum of KK's Object 1, which is listed in Table 3 as −42.6,+29.3, was obtained by P. Osmer with the cryogenic camera on the KPNO 4 m telescope in 1987 May. This spectrum has a resolution of 30 Å, and signal-to-noise ratio of 20 near 7000 Å. No strong absorption or emission lines were detected. The shape of the spectrum, along with its brightness and its chance appearance in our R frame, are consistent with its being a weak-lined G or K dwarf star.

d) Radio Emission

The field around IRAS 09104+4109 was observed in snapshot mode at the VLA[3] in 1986 August using the B-array at 6

---

[3] The VLA is operated by Associated Universities, Inc., under contract with the National Science Foundation.

and 20 cm. Figure 4 shows the 6 cm map which was produced with a 1$\rlap{.}''$5 FWHM beam. Two sources are seen: the southern source coincides with Object 2 to within 1″, while the weaker, northern source has no counterpart on the R band image. The apparent extension of the sources along the line that joins them is almost certainly spurious; there is no strong evidence that the sources are extended on a scale larger than 1″. The flux densities of the source coincident with Object 2 are included in Table 1. The radio measurement of its position is included in Table 2.

e) X-Ray Emission

No *Einstein* observations of the field of IRAS 09104+4109 are available (C. Jones, private communication).

III. RESULTS

KK's Object 2 is now unambiguously identified with IRAS 09104+4109 from ground-based infrared photometry. Its redshift, 0.442, is the largest of any object yet found as a result of the *IRAS* survey. The data summarized above suggest a classification for this object among known types of luminous extragalactic sources and permit us to address the issue of the mechanism generating its enormous infrared luminosity. The analysis below is based on the assumptions $H_0 = 100$ km s^{-1} Mpc^{-1} and $q_0 = 0.5$. Quantities sensitive to these values are parameterized by the variable $h = H_0/100$ km s^{-1} Mpc^{-1}.

a) Morphology

This object is clearly extended in our continuum R image. The measured 12″ radial extent of this source corresponds to a linear dimension of 80 h^{-1} kpc in the rest frame of the source. This envelope size ranks IRAS 09104+4109 as a cD galaxy (Matthews, Morgan, and Schmidt 1964).

Fine structure can be seen in both the continuum and emission-line images. In particular, a second peak in the emission-line surface brightness is seen ~4″ from the position of maximum brightness toward P.A. 25°. This secondary peak is also seen at lower contrast in the R frame; thus the equivalent width of the line must be higher at the position of the secondary peak than at the center of the galaxy. The similarity in emission-line width between this secondary peak and the core of the galaxy suggests that it may be the remnant of an interacting galaxy, analogous to the compact companions to QSOs found by Stockton (1982). Further support for this hypothesis comes from the observed increase in excitation of the ionized gas, as measured by the ratio [O III]/Hβ, which is highest at the position of the secondary maximum.

The only information about infrared morphology comes from a comparison of the *IRAS* with the IRTF flux densities in the 10–25 μm range. Because of the different passbands of the *IRAS* and IRTF systems a correction for the energy distribution must be applied. If we assume a $v^{-1.4}$ spectral index variation in this range, the ratio of 10 μm IRTF to 12 μm *IRAS* flux densities in Table 1 indicates that 70% ± 20% of the 8–15 μm luminosity and 95% ± 20% of the 20–25 μm luminosity of IRAS 09104+4109 originates from the central 8″ (50 h^{-1} kpc) region of the galaxy. The observations are thus compatible with a pointlike morphology for IRAS 09104+4109, but do not usefully constrain its physical size on a galactic scale.

The radio morphology of the source is peculiar. Two point sources are found in the field, one of which is coincident, within the uncertainties of the measurements, with the optical cen-
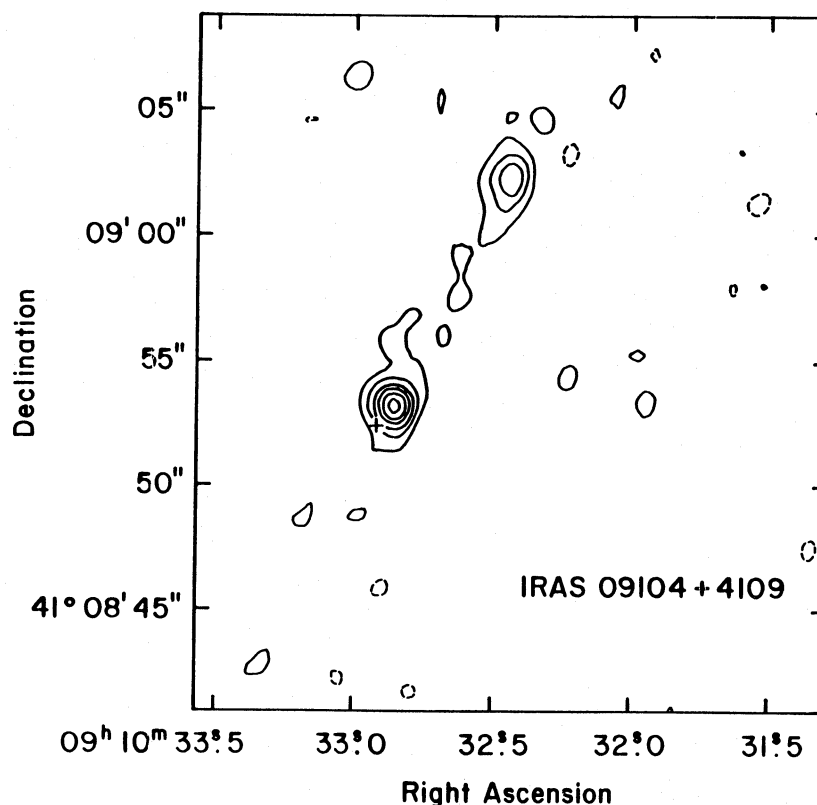
FIG. 4.—The VLA 6 cm map of IRAS 09104+4109. The contour interval is 0.2 mJy. Negative contours are dashed and the zero-level contour is omitted. The beam is approximately a circular Gaussian with FWHM of 1″.5. The cross marks the optical center of the galaxy. A weaker radio source, located at $9^h 10^m 32^s.45$, $+41°09'02″.2$, is observed at a flux level of 1.3 ± 0.07 mJy in this 6 cm map. This source has a flux density of 2.7 ± 0.07 mJy at 20 cm.

troid of the cD galaxy, while the other lies 10″ away at P.A. 333°. The current observations do not make it clear whether the second source is physically associated with the galaxy.

b) Spectrum

Most emission-line galaxies identified among the *IRAS* sources have "starburst" or H II region spectra. Unlike these objects, IRAS 09104+4109 exhibits characteristics of Seyfert galaxies (Veilleux and Osterbrock 1987): i.e., lines representing a wide variation in ionization ([O I], [N I], [S II], along with He II, [Ne V], [Fe VII]), and a significantly higher ratio of [O III]/Hβ line intensities. The lack of broad line ($\Delta v > 1000$ km s^{-1}) components to its emission lines, and the relatively high equivalent width of the [O III] 5007 line, distinguish its spectrum as that of a Seyfert 2 nucleus or narrow line radio galaxy rather than Seyfert 1 (Osterbrock 1978, 1984).

The reddening to the gas producing the emission-line spectrum can be measured by two independent line ratios in the spectrum. Comparing the case B ratios of Hγ/Hβ and Hδ/Hβ, which are 0.47 and 0.20 respectively, with the observed ratios of 0.51 and 0.20, we deduce $E_{(B-V)} < 0.12$ mag (3 σ). Using the ratio of He II lines at 3203 Å and 4686 Å, and the relation specified by Malkan (1986), we deduce $E_{(B-V)} = 0.5$ mag. Given the uncertainty in this relation and in the line intensities, this reddening is marginally consistent with the limit deduced from the Balmer lines.

Since the line-emitting region is not heavily reddened, the very low intensity of the [O III] 3133 Å fluorescent line is noteworthy. This line is pumped by He II Lyman β, and the observed ratio of its strength to He II 4686 indicates a Bowen

efficiency of 0.064—nearly a factor of 2 lower than typically found for planetary nebulae or for Seyfert 2 galaxies. Malkan (1986) has reviewed several possible causes of such a low efficiency, including rapid expansion of the cloud producing the emission lines, and the presence of dust in the emitting-line region. The two Seyfert galaxies in his sample with the lowest Bowen efficiencies are atypical in that one is a member of an interacting system, and the other contains two closely spaced emission-line peaks.

c) Continuum

The total luminosity of IRAS 09104+4109, measured at rest frame wavelengths from 0.3 to 70 μm, is $6 \times 10^{12} L_\odot h^{-2}$. This luminosity is higher than that of any previously known Seyfert 2 galaxy. The next most luminous Seyfert 2 now known was also discovered in the *IRAS* survey (IRAS 23060+0505); it is approximately 4 times less luminous than IRAS 09104+4109 (Hill, Wynn-Williams, and Becklin 1987).

Almost all of the energy of IRAS 09104+4109 is emitted between 5 and 60 μm. More than 100 times more energy is emitted at $\lambda > 1$ μm as is radiated at wavelengths between 0.3 and 1 μm, as measured in the galaxy's rest frame. [A quantity often referenced in discussions of infrared-bright galaxies is the ratio $\nu L_\nu(80)/\nu L_\nu(B)$. This ratio is less useful for IRAS 09104+4109, because much of the infrared luminosity of this galaxy emerges at wavelengths less than 80 μm.] The observed ratio of infrared to optical luminosity for IRAS 09104+4109 is intermediate between the most extreme values found for some starburst nuclei detected by *IRAS* and

the more moderate values found for QSOs (Neugebauer *et al.* 1986).

It is unlikely that the infrared continuum is produced by a nonthermal emission mechanism. First, the continuum is strongly curved between near-infrared and radio wavelengths. This fact does not rule out nonthermal mechanisms but imposes strict constraints. Second, the agreement between the ground-based infrared flux measurements and the *IRAS* measurements provides no evidence for variability, whereas, if the source had a typical brightness temperature of 10^{12} K, then its size would be only 1 lt-day across. Third, the continuum of a self-absorbed homogeneous nonthermal source drops too steeply to account for the radio *and* infrared emission; while an inhomogeneous source could match the continuum over this wavelength range, it would be even smaller than a homogeneous source (Ennis, Neugebauer, and Werner 1982).

On the other hand, thermal models may plausibly account for the infrared continuum. In this class of models, the observed decrease in flux density longward of the rest wavelength of 40 μm implies that the radiating material has a temperature of at least 120 K, which is hotter than the color temperatures of typical *IRAS* galaxies (Smith *et al.* 1987), but is commonly observed among QSOs and Seyfert galaxies detected by *IRAS* (de Grijp *et al.* 1985; Neugebauer, Soifer, and Miley 1985; Neugebauer *et al.* 1986). The high temperature of the dust implies that the size of the radiating volume and the total mass of radiating material are small. With the assumption that the dust is optically thin near the peak of the spectral energy distribution at 40 μm, and using optical constants given in Draine and Lee (1984), we derive a modest total mass of interstellar matter of $2 \times 10^7 \, M_\odot \, h^{-2}$, and an equilibrium size of 130 h^{-1} pc for the warm material. These values are consistent with the parameters of regions producing the narrow emission lines in Seyfert nuclei.

Though the optical luminosity of IRAS 09104+4109 is much lower than its infrared luminosity, it is high by comparison to other infrared-bright galaxies. The monochromatic *continuum* flux density listed in Table 1 at 0.44 μm corresponds to an absolute blue magnitude of $-21.6 + 5 \log h$, which is 3 σ greater than the average absolute blue magnitude of the galaxies in the flux-limited sample studied by Smith *et al.* (1987). On the other hand, the monochromatic *continuum* flux density at 0.55 μm corresponds to an absolute visual magnitude of $-22 + 5 \log h$, which is within the range found by Oemler (1976) for cD galaxies, if his luminosities are rescaled to our assumed cosmological constants. The detection of Ca II K in absorption confirms that most of the emission at this wavelength is due to starlight, as in other cD galaxies.

At rest wavelengths shorter than 4000 Å and longer than 1 μm, the observed continuum significantly exceeds the integrated continuum of stars found in a normal elliptical galaxy (e.g., Hamilton and Keel 1987). The short wavelength excess (apparent as a flattening of the spectrum at $\lambda < 4000$ Å in Fig. 3) is commonly seen in Seyfert galaxies (Malkan and Filippenko 1983), and has been attributed to a blend of Balmer lines and the Balmer continuum (Malkan and Sargent 1982). A near-infrared excess—amounting to a factor of 10 at 2.2 μm— has also been seen in Seyfert galaxies. This emission cannot be attributed to obscured starlight, unless the stellar luminosity of IRAS 09104+4109 greatly exceeds that of other cD galaxies. Further, the presence of excess emission at wavelengths as short as 1 μm also suggests that it is not emission from hot dust, unless the dust is subject to considerable nonequilibrium

heating of the kind described by Sellgren (1984). Thus the most likely mechanism for the near infrared emission is nonthermal emission which is presumably associated with the same object that powers the far-infrared source. Malkan and Filippenko (1983) give arguments which also favor this interpretation for the near-infrared continuum of Seyfert galaxies.

The luminosity of IRAS 09104+4109 at 6 cm is $7.5 \times 10^{23} \, h^{-2}$ W Hz^{-1}. Although this is not as luminous as the classical radio galaxies (Peacock and Wall 1981), it is more luminous than most giant elliptical galaxies; only 4% of the giant elliptical galaxies in the sample of Cordey (1986) had greater luminosities. There is a strong correlation between far-infrared luminosity and radio luminosity for *IRAS* galaxies (Helou, Soifer, and Rowan-Robinson 1985; Eales, Wynn-Williams, and Beichman 1987). IRAS 09104+4109 appears to have about 10 times more far-infrared emission than would be expected from its radio emission compared with most *IRAS* galaxies, but because of the uncertainty in the slope of the far-infrared–radio relationship, the dispersion in the relationship, and the extrapolation needed to reach the luminosity of this source, it is not clear whether this discrepancy is significant.

d) The Cluster

The objects in Table 3 constitute a complete sample brighter than $R = 22$ in a 6.4 square arcmin region of the sky. Kron's (1980) measurements of the surface number density of galaxies indicate that fewer than 10 galaxies brighter than this limit should be found in a random region of the sky having the same area as that represented in Table 3. We interpret the overdensity of sources in the vicinity of IRAS 09104+4109 as a cluster of galaxies physically associated with it.

To test this hypothesis, we compare the color-magnitude ($R-I$ vs. R) diagram of objects in Table 3 with a similar diagram for the cluster Cl 0024+1654, which lies at $z = 0.392$. Photometry for members of this latter cluster was obtained by Schneider, Dressler, and Gunn (1986, hereafter SDG), using the *gri* photometric system. A transformation from that system to the *RI* Kron-Cousins system used here was performed by adopting the conversion to the Johnson *RI* system from Wade *et al.* (1979) and then the conversion to the Kron-Cousins system from Bessell (1979). Prior to performing these transformations, the data of SDG were first redshifted from $z = 0.392$ to $z = 0.442$ based on the *K*-corrections of Schneider, Gunn, and Hoessel (1983). This amounts to a $(r - i)$ color change of <0.05 magnitudes.

The color-magnitude diagram for the two clusters are presented in Figure 5. All objects which are definitely known not to be cluster members (by spectroscopic observations) were excluded. The similarity of the diagrams for the two clusters implies that most of the objects in the field of IRAS 09104+4109 lie at approximately the same redshift as that of the cD galaxy. Alternatively, the luminosity function as projected in these diagrams are approximately equal, when scaled by the cluster population. The points which are not within the envelope defined by Cl 0024+1654 are probably misclassified stars.

Assuming that all of the objects in Table 3, except those known to lie at different redshifts, are galaxies in a cluster associated with IRAS 09104+4109, we can estimate details of the cluster's structure. First, its extent is at least as large as the field covered by our *R*-band image, i.e., 3', or 1 h^{-1} Mpc at the distance to the cluster. This value is about equal to twice the
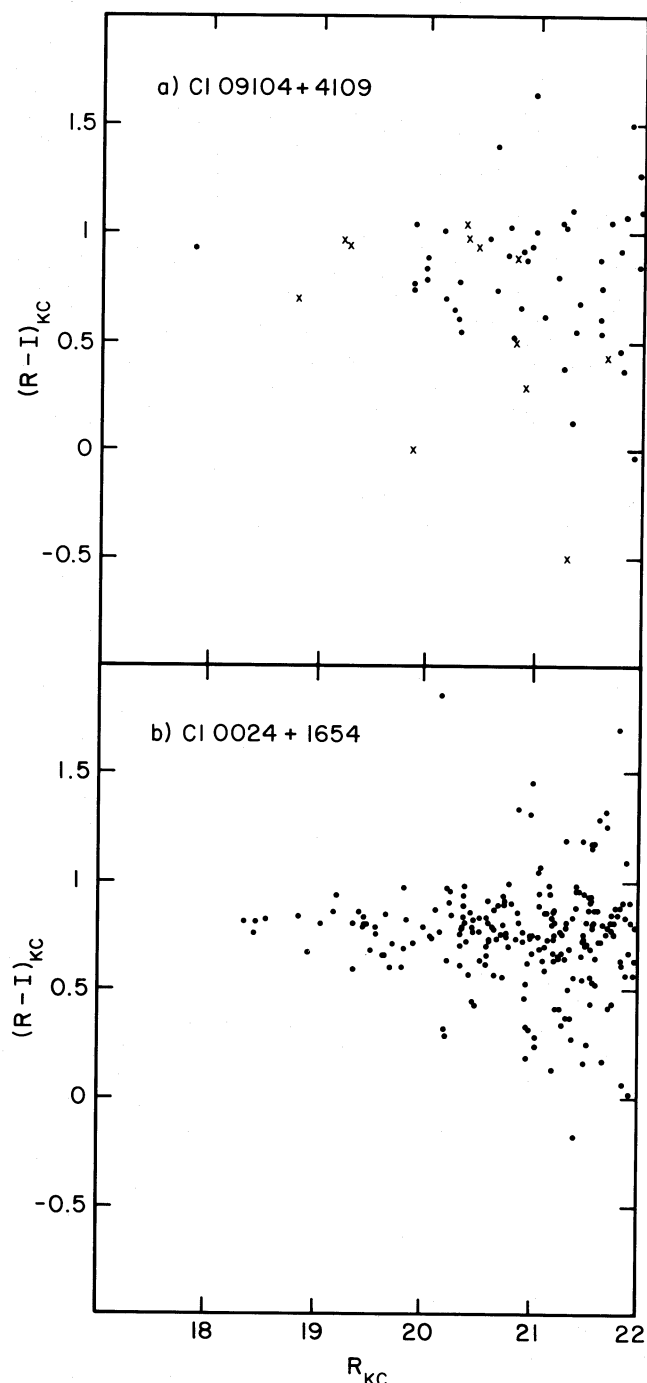
FIG. 5.—Color-magnitude diagrams for the objects listed in Table 3 (excluding objects known not to be associated with IRAS 09104+4109) and the cluster Cl 0024+1654. The photometry of sources indicated by an "X" in (*a*) is uncertain due to confusion. The catalog of galaxies in Cl 0024+1654 cover an area that is 4.5 times greater than the area covered by the listed in Table 3; thus the two clusters have a comparable richness.

core radius of a rich cluster, but is ∼5 times the core radius found by SDG for Cl 0024+1654. The data presently available indicate that the cluster center lies 26″ west of IRAS 09104+4109, similar to the offset of the cD galaxy in Cl 0024+1654 from its cluster center (SDG).

The overall shape of the cluster appears flattened, unlike that of Cl 0024+1654 (SDG). The axial ratio, defined by

Adams, Strom, and Strom (1980), as the average ratio of the offset from the cluster center (assumed to be the cD galaxy) along the *major* axis to the offset along the *minor* axis, is 0.76; this is somewhat higher than the axial ratios of the linear clusters studied by those authors. However, we note that this value is highly uncertain, as it is sensitive to the offset of the cD galaxy from the cluster center. As an alternative measure of the cluster shape, we have computed the root sum squares of the difference in position of each object in Table 3 from the projected *major* and *minor* axes. The ratio of these quantities is 0.5. No difference in this ratio is obtained by considering only the galaxies brighter than the median of our sample.

IV. DISCUSSION

IRAS 09104+4109 has been identified with a cD galaxy having a rich Seyfert 2–like emission-line spectrum at a redshift of $z = 0.442$. Its total luminosity is $6 \times 10^{12} L_\odot h^{-2}$, which is higher than any other object discovered as a result of the *IRAS* survey, and higher than any other galaxy in its spectroscopic or morphological class. What makes this galaxy so much more luminous than other objects to which it might be compared on the basis of its spectrum or morphology? The only other extragalactic objects now known with higher infrared luminosities than IRAS 09104+4109 are all classified as Seyfert 1 or QSO (Neugebauer *et al.* 1986). Yet no broad-line region is visible in spectra now available for IRAS 09104+4109, which would link it to the Seyfert 1/QSO class of objects. As Hill, Wynn-Williams, and Becklin (1987) suggested in the case of the Seyfert 2 galaxy IRAS 23060+0505, the broad-line region of IRAS 09104+4109 may be obscured by the same dust producing its enormous infrared luminosity. The unreddened emission-line spectrum of IRAS 09104+4109 then requires an incomplete covering factor for the dust-filled region. This factor was estimated using the treatment given in Osterbrock (1974), assuming (*a*) all of the Lyman continuum photons that are impinging on the $H\beta$ emitting region are absorbed in it, (*b*) the temperature of the gas producing the $H\beta$ line is 10,000 K (in which case each $H\beta$ photon represents 12.8 Lyman continuum photons), and (*c*) the continuum of the ionizing source is flat [i.e., $F(v) \sim v^0$] between the H^0 and He^0 Lyman limits. The derived Lyman continuum luminosity associated with the observed $H\beta$ emission is only $1.4 \times 10^{11} L_\odot$, or 2% of the total observed luminosity of IRAS 09104+4109, indicating that the dust producing the infrared emission covers 98% of the central source.

Besides understanding what type of source powers the luminosity of IRAS 09104+4109, it is important to understand what phenomenon triggered its current outburst. Its location in a rich cluster suggests that the outburst might have resulted from an interaction with a cluster member. The secondary peak seen in the emission-line image of this galaxy, which has lines as broad as those seen in the central peak, may be the remnant of the intruding galaxy. However, other well-studied cluster-center galaxies, such as Cyg A and NGC 1275, which also have emission-line spectra resembling Seyferts, and also exhibit evidence for recent interactions with other galaxies in their clusters (Pierce and Stockton 1986; Hu *et al.* 1985), have 50–100 times lower bolometric luminosity than IRAS 09104+4109. This poses the question whether the large difference in luminosity between these galaxies and IRAS 09104+4109 is due to differences in the gas contents of the intruding galaxies, the properties of the nonthermal sources at their centers, or the histories of the interactions.

V. CONCLUSIONS

In this paper we have shown that the galaxy associated with *IRAS* source IRAS 09104+4109 is remarkable for the following reasons.

1. It is the most distant ($z = 0.442$) and the most luminous ($6 \times 10^{12}\ L_\odot\ h^{-2}$) object discovered as a result of the *IRAS* survey. Only a few previously cataloged quasars have higher IR luminosities.

2. It is identified with a cD galaxy which lies in a rich, flattened, cluster of galaxies. In the list of cD galaxies given by Matthews, Morgan, and Schmidt (1964) only Cyg A was detected in the *IRAS* survey, and it has far lower infrared luminosity than IRAS 09104+4109.

3. Ninety-nine percent of its luminosity is emitted longward of 1 μm. The energy distribution in the 25–60 μm range is unusually "warm" for a galaxy in the *IRAS* catalog.

4. The optical spectrum of its nucleus resembles that of a Seyfert 2 or narrow line radio galaxy; no evidence for quasar-like broad emission lines is seen.

5. It is associated with a pair of radio sources, one of which coincides with the galaxy nucleus, the other of which lies about 70 h^{-1} kpc away.

REFERENCES

Adams, M. T., Strom, K. M., and Strom, S. E. 1980, *Ap. J.*, **238**, 445.
Bessell, M. S. 1979, *Pub. A.S.P.*, **91**, 589.
Cohen, R. D., and Osterbrock, D. E. 1981, *Ap. J.*, **243**, 81.
Cordey, R. A. 1986, *M.N.R.A.S.*, **219**, 575.
Davis, L. E., Cawson, M., Davies, R. L., and Illingworth, G. 1985, *A.J.*, **90**, 169.
DeGrijp, M. H. K., Miley, G. K., Lub, J., and DeJong, T. 1985, *Nature*, **314**, 240.
Draine, B. T. and Lee, H. M. 1984, *Ap. J.*, **285**, 89.
Eales, S. A., Wynn-Williams, C. G., and Beichman, C. A. 1988, *Ap. J.*, **328**, in press.
Ennis, D. J. Neugebauer, G., and Werner, M. 1982, *Ap. J.*, **262**, 460.
Hamilton, D., and Keel, W. C. 1987, *Ap. J.*, **321**, 211.
Helou, G., Soifer, B. T., and Rowan-Robinson, M. 1985, *Ap. J. (Letters)*, **298**, L7.
Hill, G. J., Wynn-Williams, C. G., and Becklin, E. E. 1987, *Ap. J. (Letters)*, **316**, L11.
Houck, J. R., Schneider, D. P., Danielson, G. E., Beichman, C. A., Lonsdale, C. J., Neugebauer, G., and Soifer, B. T. 1985, *Ap. J. (Letters)*, **290**, L5.
Hu, E. M., Cowie, L. L., Kaaret, P., Jenkins, E. B., York, D. G., and Roesler, F. L. 1983, *Ap. J. (Letters)*, **275**, L27.
IRAS Point Source Catalog. 1985, Joint *IRAS* Science Working Group (Washington D.C.: U.S. Government Printing Office).
Kleinmann, S. G., and Keel, W. C. 1987, in *Star Formation in Galaxies*, ed. Carol J. Lonsdale Persson (NASA C.P. 2466), p. 559 (KK).
Kron, R. G. 1980, *Ap. J. Suppl.*, **43**, 305.
Landolt, A. 1983, *A.J.*, **88**, 434.
Low, F. J., *et al.* 1984, *Ap. J. (Letters)*, **278**, L19.
Malkan, M. A. 1986, *Ap. J.*, **310**, 679.
Malkan, M. A., and Filippenko, A. V. 1983, *Ap. J.*, **275**, 492.
Malkan, M. A., and Sargent, W. L. W. 1982, *Ap. J.*, **254**, 22.

Matthews, T. A., Morgan, W. W., and Schmidt, M. 1964, *Ap. J.*, **140**, 35.
Neugebauer, G., Miley, G. K., Soifer, B. T., and Clegg, P. E. 1986, *Ap. J.*, **308**, 815.
Neugebauer, G., Soifer, B. T., and Miley, G. K. 1985, *Ap. J. (Letters)*, **295**, L27.
Oemler, A., Jr. 1976, *Ap. J.*, **209**, 693.
Oke, J. B., and Gunn, J. E. 1983, *Ap. J.*, **266**, 713.
Osterbrock, D. E. 1974, *Astrophysics of Gaseous Nebulae* (San Francisco: Freeman).
———. 1978, *Proc. Natl. Acad. Sci.*, **75**, 540.
———. 1984, *Quart. J.R.A.S.*, **25**, 1.
Osterbrock, D. E. and Miller, J. S. 1975, *Ap. J.*, **197**, 535.
Peacock, J. A., and Wall, J. V. 1981, *M.N.R.A.S.*, **194**, 331.
Pierce, M. J., and Stockton, A. 1986, *Ap. J.*, **305**, 204.
Schmidt, G. D., and Miller, J. S. 1985, *Ap. J.*, **290**, 517.
Schneider, D. P., Dressler, A., and Gunn, J. E. 1986, *A.J.*, **92**, 523 (SDG).
Schneider, D. P., Gunn, J. E., and Hoessel, J. G. 1983, *Ap. J.*, **264**, 337.
Sellgren, K. 1984, *Ap. J.*, **277**, 623.
Smith, B. J., Kleinmann, S. G., Huchra, J. P., and Low, F. J. 1987, *Ap. J.*, **318**, 161.
Stockton, A. 1982, *Ap. J.*, **257**, 33.
Valdes, F. 1982a, in *Instrumentation in Astronomy IV*, ed. D. Crawford (*Proc. SPIE*, **331**), p. 465.
———. 1982b, *FOCAS, Faint Object Classification and Analysis System* (KPNO User's Manual).
———. 1986, in *Instrumentation in Astronomy VI*, ed. D. Crawford (*Proc. SPIE*, **627**), p.749.
Veilleux, S., and Osterbrock, D. E. 1987, *Ap. J. Suppl.*, **63**, 295.
Wade, R. A., Hoessel, J. G., Elias, J. H., and Huchra, J. P. 1979, *Pub. A.S.P.*, **91**, 35.

E. E. BECKLIN, S. A. EALES, K. D. KUNTZ, and C. G. WYNN-WILLIAMS: Institute for Astronomy, University of Hawaii, 2680 Woodlawn Drive, Honolulu, HI 96822

DONALD HAMILTON: National Optical Astronomy Observatories, P.O. Box 26732, Tucson, AZ 85726-6732

W. C. KEEL: Sterrewacht Leiden, Postbus 9513, 2300 RA Leiden, Nederland

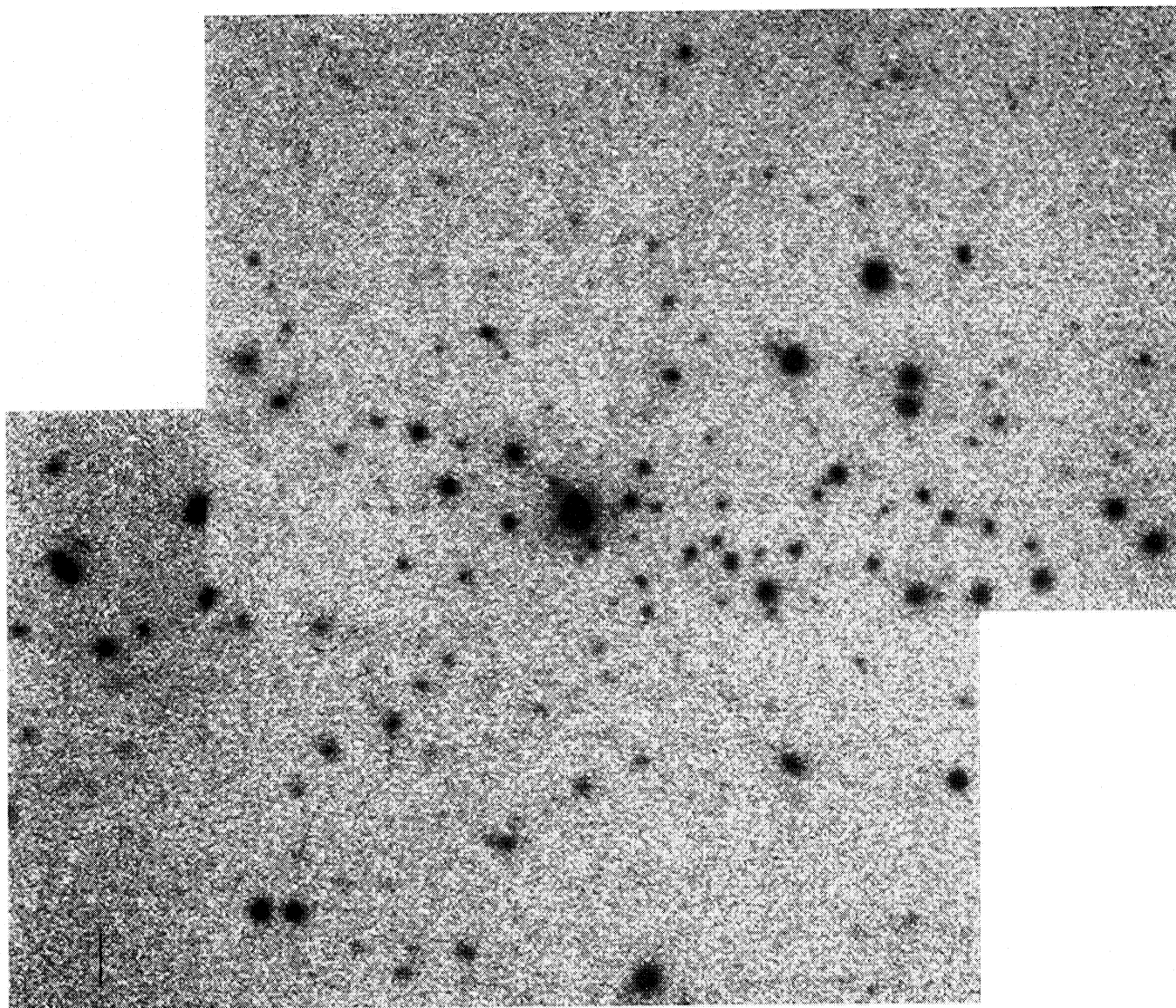S. G. KLEINMANN: 619 Graduate Research Center, University of Massachusetts, Amherst, MA 01003

PLATE 5

FIG. 1.—A mosaic of two short exposure (600 s) R band images of the field surrounding IRAS 09104 + 4109. Both images were median filtered to remove cosmic rays. North is at the top and east is to the left. The vertical line on the lower left side represents 10″. The bright galaxy at the center is Kleinmann and Keel's Object 2, now unambiguously identified with IRAS 09104 + 4109.

KLEINMANN et al. (see 328, 162)